Proteomic Profile of TGF-β1 treated Lung Fibroblasts identifies Novel Markers of Activated Fibroblasts in the Silica Exposed Rat Lung

Mao Na[1*], Xu Hong[2*], Jin Fuyu[1], Xu Dingjie[3], Dominic Sales[4], Zhang Hui[1], Wei Zhongqiu[1], Li Shifeng[2], Gao Xuemin[2], Cai Wenchen[5], Li Dan[1], Zhang Guizhen[1], Zhang Bonan[5], Zhang Lijuan[2], Li Shumin[5], Zhu ying[5], Wang Jin[1], Rui Mingwang[2], Ross Summer[4], Yang Fang[1,5#],

1. Basic Medical College, North China University of Science and Technology, Tangshan, China
2. Medical Research Center, North China University of Science and Technology, Tangshan, Chin a
3. College of Traditional Chinese Medicine, North China University of Science and Technology, Tangshan, China
4. Center for Translational Medicine, Jane and Leonard Korman Respiratory Institute, Thomas Jefferson University, Philadelphia, PA, USA
5. School of public health, North China University of Science and Technology, Tangshan, China

*co-first author

[#]corresponding author:
Fang Yang, M.D.
Basic Medical College, North China University of Science and Technology
No. 21 Bohai Road, Caofeidian Eco-city, Tangshan city, Hebei province 063000, China
Email: fangyang990404@sina.com

ABSTRACT: We performed liquid chromatography-tandem mass spectrometry (LC-MS/MS) on control and TGF-β1-exposed rat lung fibroblasts to identify proteins differentially expressed between cell populations. A total of 1648 proteins were found to be differentially expressed in response to TGF-β1 treatment and 196 proteins were expressed at ≥ 1.2 fold relative to control. Guided by these results, we next determined whether similar changes in protein expression were detectable in the rat lung after chronic exposure to silica dust. Of the five proteins selected for further analysis, we found that levels of all proteins were markedly increased in the silica-exposed rat lung, including the proteins for the very low density lipoprotein receptor (VLDLR) and the transmembrane (type I) heparin sulfate proteoglycan called syndecan 2 (SDC2). Because VLDLR and SDC2 have not, to our knowledge, been previously linked to the pathobiology of silicosis, we next examined whether knockdown of either gene altered responses to TGF-β1 in MRC-5 lung fibroblasts. Interestingly, we found knockdown of either VLDLR or SDC2 dramatically reduced collagen production to TGF-β1, suggesting that both proteins might play a novel role in myofibroblast biology and pathogenesis of silica-induced pulmonary fibrosis. In summary, our findings suggest that performing LC-MS/MS on TGF-β1 stimulated lung fibroblasts can uncover novel molecular targets of activated myofibroblasts in silica-exposed lung.

Key words: proteomics; fibroblast; silicosis; lung; pulmonary fibrosis

48

49 **Highlights:**

50 We identified 196 proteins differentially expressed between control and TGF-β1
51 treated fibroblastsby LC-MS/MS.

52 Several proteins identified by LC-MS/MS were also found to be differentially
53 expressed in whole lung tissues and isolated fibroblasts after chronic exposure to
54 silica dust, including the very low density lipoprotein receptor (VLDLR) and the
55 transmembrane type I heparan sulfate proteoglycan called syndecan 2

56 Knockdown of SDC2 or VLDLR markedly inhibited collagen production in MRC-5
57 fibroblasts, suggesting a novel pathogenic role for these proteins in myofibroblast
58 biology.

INTRODUCTION

Silicosis is a highly prevalent occupational condition that is caused by chronic inhalation of crystalline silica particulates (aerodynamic diameter < 5 μm) into the distal air spaces of the lung. Though this disease is largely preventable by implementing strict safety and health standards at work, silicosis remains one of the more common occupational disorders in many parts of the world, including China.

Although silica dust has been shown to injure many cell types in the lung it is generally believed that activated myofibroblasts play a central role in driving the development of disease. Central to this activation is signaling through the transforming growth factor β1 (TGF-β1) receptor, which leads to a cascade of events that trigger the transdifferentation of fibroblasts to myofibroblasts and induce the production of large quantities of collagen and other extracellular matrix materials (Gauldie *et al.*, 1999; Harris *et al.*, 2013; Jagirdar *et al.*, 1996). Despite decades of work on TGF-β1 signaling in lung fibroblasts much remains to be learned about molecular mechanisms controlling myofibroblast growth and activation. Moreover, it is largely believed by many experts in the field that gaining additional insight into biological events downstream of TGF-β1 signaling could lead to the identification of new molecular targets for the treatment of silicosis and various other fibrotic lung conditions.

In our previous work, we utilized a 2-DE proteomic approach to identify novel biomarkers of silicosis (Xiaojun *et al.*, 2016). However, it is now clear that using isobaric tags for relative quantification (iTRAQ) has several advances over the 2-DE approach including higher throughput quantification, decreased analytical time, and lower run-to-run variation (Rauniyar *et al.*, 2014). With this in mind, the objective of this work was to utilize iTRAQ coupled liquid chromatography-tandem mass spectrometry (LC-MS/MS) to identify novel markers of activated rat lung fibroblasts and to utilize this information to assess whether similar markers were upregulated in the rat lung after chronic exposure to silica dust.

MATERIALS AND METHODS

Cell culture. Rat lung fibroblasts were isolated from 1–3 day old Wistar rats as previously described (Xu *et al.*, 2012). Briefly, freshly isolated cells were culture for 3 to 4 passages and then transferred to low serum conditions (0.5% FBS) for 24 h. Following serum deprivation, cellwere treated with 5 ng/ml TGF-β1 (240-B; R&D Systems, Inc., Minneapolis, MN, USA) or vehicle controlfor 24 h and whole cell lysates were collected for later analysis (Xiaojun, et al., 2016). For each group, cells from 10 independent samples were pooled for proteomics analysis.

Fibroblasts used in our studies were derived from the lungs of control and silica-exposed rats(Seluanov *et al.*, 2010) and the MRC-5 cell line. Fibroblasts were cultured in MEM containing 2% HEPES, 1% nonessential amino acid, and 10% FBS. Transient transfections were carried out using lipofectamine 2000 (Invitrogen, USA) according to the manufacturer's recommendations. Knockdown was performed by exposing MRC-5 cells to 10 ng of siRNA targeting either very low-density lipoprotein receptor (VLDLR) or syndecan-2 (SDC2). Six hours after transfection, cells were washed and exposed to medium containing vehicle control or TGF-β1.

siRNAs used in our studies were derived from following sequences: 1) VLDL R-siRNA 1: GUGCAACAAUGGCCAGUGU dTdT; CACGUUGUUACCGGUCA CA dTdT; 2) VLDLR-siRNA 2: GCGAGUGCAUCCAUAAGAA dTdT; CGCU CACGUAGGUAUUCUU dTdT; 3) VLDLR-siRNA 3: GAUCGACAAUGUCUA UAAU dTdT; CUAGCUGUUACAGAUAUUA dTdT; 4) SDC2-siRNA 1: CCA CGACGCUGAAUAUACA dTdT; GGUGCUGCGACUUAUAUGU dTdT; 5) SD C2-siRNA 2: GUUGGUGUAUCGCAUGAGA dTdT; CAACCACAUAGCGUAC UCU dTdT; 6) SDC2-siRNA 3: GGAGAACGCAAACCAUCCA dTdT; CCUCU UGCGUUUGGUAGGU dTdT.

Sample preparation for LC-MS/MS analysis. Proteins for LC-MS/MS were as prepared previously described (Wisniewski *et al.*, 2009)(Promega, Fitchburg, Wisconsin, USA). Briefly, cell lysates were loaded onto a 10-kDa filter unit (Pall Corp., Port Washington, New York, USA), and filter was sequentially washed with

UA (8 M urea in 0.1 M Tris-HCl;pH 8.5) and ABC (25 mMNH_4HCO_3) buffers. Proteins in collected samples were then denatured in 20 mM DTT at 50°C for 1 h and carboxyamidomethylated with 50 mM iodoacetamide (IAA) for 45 min. This step was followed by a digestion step using Trypsin Gold (1:50) at 37°C overnight. Peptide fragments were next desalted using Oasis HLB cartridges (Waters, Milford, Massachusetts, USA), dried by vacuum centrifugation (Thermo Fisher Scientific, Bremen, Germany) and again collected as a filtrate. Finally, samples were labelled with 4-plex iTRAQ reagent (AB Sciex) according to the manufacture's protocol, with the control group labelled with tag 116 and TGF-β group with tag 117.

High-performance liquid chromatography (HPLC) separation. Pooled mixtures of labelled samples were fractionated using a high-pH HPLC on a Waters Xbridge C18 column (4.6 mm × 250 mm, 3 μm). Samples were loaded onto a column equilibrated in buffer A1 (H_2O; pH10), with an elution gradient of 5 – 25% buffer B1 (90% ACN; pH10) and a flow rate = 1 mL/min for 60 min. Flow-through was collected at 1minute intervals for a total of 60 fractions. Solutions were then dried, re-suspended in 0.1% formic acid, and pooled by concatenating fractions 1, 31; 2, 32; and so on. Analyses were performed on just odd number fractions.

LC-MS/MSanalysis. Each fraction was analysed with a reverse-phase-C18 self-packed capillary LC column (75 μm × 100 mm), with an elution gradient of 5% – 30% buffer B2 (0.1% formic acid, 99.9% ACN; flow rate = 0.3 μL/min) for 40 min. A Triple TOF 5600 mass spectrometer was used to analyze the eluted peptides, with each fraction run in duplicate. The MS data were acquired using the high-sensitivity mode with the following parameters: 30 data-dependent MS/MS scans per full scan; full scans acquired at a resolution of 40,000 and MS/MS scans at a resolution of 20,000; rolling collision energy, charge state screening (including precursors with a charge state of +2 to +4), and dynamic exclusion (exclusion duration 15 s); and a MS/MS scan range of 100 – 1800 m/z, with a scan time of 100 ms.

Date analysis. Data acquired from LC-MS/MS were analysed using the Mascot software (version 2.4.1, Matrix Science, London, UK). Proteins were identified by

146 searching peptide spectral matches against the Swissprot_2014_07 database
147 (taxonomy: Rattus, containing 7,906 sequences). The parameters utilized included
148 trypsin as the digestion enzyme, two or fewer missed cleavage sites and cysteine
149 carbamidomethylation (57.02146) as a fixed modification. The precursor ion mass
150 tolerance and the fragment ion mass tolerance were set to ppm and 0.05 Da
151 respectively. Protein identifications from Mascot were validated using the Scaffold
152 Proteome Software (version 4.3.3, Proteome Software Inc., Portland, OR). Peptide
153 identifications were accepted if false discovery rate (FDR) was less than 1.0% and if
154 at least 2 unique peptides were identified from the same protein. iTRAQ, Scaffold Q+
155 was used for Label Based Quantification (TMT, iTRAQ, SILAC, etc.) of peptides and
156 proteins. For each channel, the acquired reporter ion intensities were normalized by
157 the sum of all reporter ion intensities of that channel. Normalized intensities were then
158 used to calculate the relative protein abundance and quantify protein
159 ratios(Nesvizhskii *et al.*, 2003). Proteins identified from these analyses were further
160 analysed to determine function, ontology and location using the PANTHER
161 classification system (Protein Analysis Through Evolutionary Relationships;
162 http://www.pantherdb.org/) (Mi *et al.*, 2013).

163 **Silicosis model.** Male Wistar rats were purchased from Vital River Laboratory Animal
164 Technology Co. Ltd. (SCXY 2009-0004; Beijing, China) and all experiments were
165 performed in accordance with the regulations set by the Committee on the Ethics of
166 North China University of Science and Technology. Silica dust was delivered to rats
167 using a HOPE MED 8050 exposure control apparatus (HOPE Industry and Trade Co.
168 Ltd, Tianjin, China) with the SiO_2(s5631, Sigma-Aldrich, St. Louis, MO, USA)
169 concentration maintained at 2,000 mg/m^3 (Liu *et al.*, 2017). At experimental endpoints,
170 bronchoalveolar lavage was performed with 0.9% saline and whole lung tissues were
171 then snap-frozen in liquid nitrogen.

172 **Immunohistochemistry (IHC).**Paraffin-embedded tissue sections were used for IHC.
173 Endogenous peroxidases were quenched with 3% H_2O_2 and antigen retrieval was
174 performed using a high-pressure method with deparaffinised sections. The samples

were then incubated with primary antibodies against collagen V(COL V, A1515, ABclonal Biotech, Wuhan, China), collagen XI (COL XI, DF3553, Affinity Biosciences, Cincinnati, OH, USA), VLDLR (TA309928, OriGene Technologies, Rockville, MD, USA) or SDC2 (A1810, ABclonal Biotech, Wuhan, China) at 4°C overnight. The following morning, tissue sections were incubated with secondary antibody conjugated with the horseradish peroxidase enzyme (PV-6000; Beijing ZhongshanJinqiao Biotechnology Co. Ltd, China) at 37°C for 20 min. Immunoreactivity was visualised with using the DAB substrate (ZLI-9018; ZSGB-BIO, Beijing, China) and the nuclei were stained with hematoxylin.

Western blot analysis. Total protein levels were quantified using a Bradford assay (PC0020; Solarbio, China) as previously described. Protein lysates (20 μg/lane) were separated on a 13% gel by SDS-PAGE and were electro-transferred onto polyvinylidene fluoride (PVDF) membranes (Amervehicle Biosciences). The membranes were blocked with 5% non-fat milk and incubated with primary antibodies against COL V, COL XI, Vascular cell adhesion protein (VCAM, ab134047, Abcam, Cambridge, MA, USA), Transmembrane protein 214 (TM214, TS306822, OriGene Technologies, Rockville, MD, USA), VLDLR, SDC-2 or α-SMA at 4°C overnight. Membranes were next washed in TBST and incubated with peroxidase-labelled affinity-purified anti-rabbit/mouse IgG (H + L) secondary antibody(074–1506/074–1806;Kirkegard and Perry Laboratories). Protein bands were visualised using ECL™ Prime Western Blotting Detection Reagent (RPN2232; GE Healthcare, Hong Kong, China) and expressed as a fold change relative to α-Tubulin (Tub α, AF7010; Affinity Biosciences, Cincinnati, OH, USA).

Statistical analysis. Comparisons between two groups were performed using independent sample *t*-test. Comparisons between multiple independent groups were done using a one-way ANOVA followed by a post-hoc analysis with the Bonferroni test. Values were expressed as a means ± Std, with p-values less than 0.05 considered as statistically significant.

RESULTS

Proteomic profile differs between control and TGF-β1 lung fibroblasts. To identify proteins differentially expressed between control and activated fibroblasts, we performed iTRAQ coupled with LC-MS/MS on rat lung fibroblasts treated with or without TGF-β1 for 24 h. Using scaffold integration, we observed a total of 1648 proteins differentially expressed between control and TGF-β1 treated cells. Moreover, 196 of these proteins were expressed at ≥ 1.2 fold-change (Tables S1 and S2) and 20 proteins exhibited a ≥ 1.5 fold-change (Table 1) relative to control.

Bioinformatic analyses of differentially expressed proteins in control and TGF-β1 stimulated lung fibroblasts. Proteins whose expression changed most significantly after exposure to TGF-β1 were classified into functional classes using the PANTHER analysis. Gene ontology (GO) analysis classified proteins into three distinct categories entitled: 1) molecular function; 2) biological process; and 3) components of the cell. Among these categories most proteins were belonged to molecular functions group (Table S3), and the major subgroups within this category included: 1) catalytic activity (40%); 2) protein binding (26%), and 3) structural activity (20%). In the biological processes category (Table S4), most proteins belonged to the subgroups: 1) cellular process (26%); 2) metabolic process (22%), or 3) cellular component/biogenesis (10%) subgroup; and proteins within the components of a cell group belonged to 1) cell part (40%); 2) cellular organelle (25%); and 3) macromolecular complexes (18%) (Table S5).

Within PANTHER, class ontology was also performed (Table S6), with the largest number of proteins assigned to the following categories:1) nucleic acid binding (18%); 2) hydrolase (10%); 3) enzyme modulator and transferase (each 7%); 4) cytoskeletal protein (6%); 5) signalling molecule (6%); and 7) transfer/carrier protein (6%). Pathway analysis showed that all proteins that were differentially expressed in response to TGF-β1fell into one of the following signalling pathways: 1) integrin; 2) angiogenesis; 3) CCKR; 4)conadotropin-releasing hormone receptor; 5) p53; 6) Alzheimer disease-presenilin; 7) blood coagulation; 8) cadherin; 9) cholesterol

biosynthesis; 10) FGF or 11) Wntsignalling pathways (Table S7).

Proteinsincreased in TGF-β1 stimulated lung fibroblasts were also increased in the silica-exposed rat lung. To determine whether in vitro findings were representative of changes in vivo, we next performed IHC and western blot analysis on control and silica-exposed lung tissues for those proteins whose expression changed most significantly (≥1.5 fold increase) in response to TGF-β1 treatment. However, our analysis was limited to proteins in which a commercially available antibody for IHC or WB was available; this included the proteins COLV, COL XI, VCAM1, TM214, VLDLR, and SDC2 for protein identification.

As shown in Figure 1A, van Gieson (VG) staining confirmed the ability of our model to induce severe fibrotic responses in the rat lung as demonstrated by an increase in extracellular matrix deposition and the large number of silicotic nodules. Western blot analysis also showed an increase in COLI and α-SMA in whole lung tissues and primary lung fibroblasts after silica exposure (Figure 1B).

As shown in Figure 2, Western blot analysis revealed a marked increase in the expression of COL V, COL XI, and VCAM1 in the lungs of silica exposed rats, including whole lung tissues and freshly isolated lung fibroblasts. Moreover, IHC staining of the lung showed the elevated levels of COL V and COL XI was confined mostly to the interstitium of the lung, particularly in areas with evidence of active inflammation and fibrosis. Despite multiple attempts, staining for VCAM1 was detected in either the control or the silica-exposed rat lung, indicating that our antibody could not be used for IHC.

In addition to the above proteins, we found that levels of VLDLR and SDC2 were also markedly increased by western blot in whole lung tissues and isolated fibroblasts after silica exposure. (Figure 3). Significant increases in VLDLR and SDC2 expression were also observed by IHC in the silica-exposed lung.

Knockdown of VLDLR or SDC2 reduces collagen deposition in TGF-β1stimulated fibroblasts. Although not entirely surprising that collagen levels

COL V and COL XL) and VCAM expression(Agassandian *et al.*, 2015) were increased in fibrotic lung tissues we were intrigued by the observation that levels of VLDLR and SDC2 were also markedly elevated in the lung after silica exposure. Even after an exhaustive search, we were unable to find any reports linking either VLDLR or SDC2 to silicosis in any tissues. Based on this, we speculated whether changes in the expression of VLDLR or SDC2 can influence fibrotic responses to TGFβ1 in lung fibroblasts. To test this, we next performed siRNA knockdown of VLDLR or SDC2 in MRC-5 cells using several different siRNA probes. Because the quantity of gene knockdown varied with different siRNAs we utilized only siRNAs demonstrating the most effective knockdown in our studies; this was siRNA 2 and 3 for VLDLR, and siRNA 3 for SDC2 (Figure 4). As shown in Figure 4, we found that knockdown of VLDLR markedly reduced COL I and α-SMA expression in TGFβ1 treated MRC-5 fibroblasts. Moreover, we also found that knockdown of SDC2 significantly suppressed COLI expression, although non-significant decreases in α-SMA levels were seen in TGFβ1 treated cells.

DISCUSSION

Biomarker discovery can be accomplished using a variety of proteomic approaches and biological specimens, including urine, serum or lysates from whole organ digests. However, for research in solid organs, such as the heart, brain, kidney or lung, it is often difficult to obtain sufficient quantities of patient samples for proteomic work. Moreover, tissue lysates, are composed of a conglomeration of different cell types, such as epithelial cells, smooth muscle cells, fibroblasts, immune cells and endothelialium, making it difficult to uncover novel biological mechanisms in individual cell types. Thus, *in vitro* models of individual cell populations are often employed to identify novel candidate biomarkers of functional processes *in vivo* (Paul *et al.*, 2013).

In this study, we performed iTRAQ-coupled LC-MS/MS analysis on rat lung fibroblasts treated with or without TGF-β1 to identify novel markers of activated myofibroblasts in the silica-exposed lung. From these studies, we identified many proteins differentially expressed and 196 proteins expressed at ≥ 1.2 fold relative to control. Importantly, many of these proteins were novel markers and had not previously been linked to TGF-β1 signalling in the lung, including several whose functional classes have been intimately tied to myofibroblast activation such as integrin and angiogenesis pathways as well as those less clearly associated with myofibroblast biology such as nucleic acid binding, hydrolase activity and transferase activity.

An important finding in this study was the observation that some of the proteins we identified in our proteomics analyses were also differentially expressed in the lung after silica exposure. For example, we found that levels of COL XI and COL V were markedly increased in the silicotic lung, although these findings were not surprising given the fact that collagen production is a well-recognized by product of TGF-β1 signalling(Raglow *et al.*, 2015). However, we also found that VCAM were significantly increased in the lung after silica exposure. The former findings is also

not unexpected given that transcript and protein levels of VCAM are reported to be increased in fibroblastic foci of IPF lungs (Agassandian, et al., 2015).

Two other proteins found to be differentially expressed in our proteomic analyses were VLDLR and SDC2. We were intrigued by these observations because our review of the literature had not previously associated these proteins with silicosis. Western blot analysis and IHC confirmed that both proteins were increased in whole lung tissues and isolated fibroblasts from the lungs of silica-exposed rats. Interestingly, VLDLR expression is known to be increased in the fibrotic caps of atherosclerotic lesions in systemic blood vessels, suggesting it may be involved in more than just lipid trafficking (Eck *et al.*, 2005). In IPF patient lung tissues, SDC2 was found to be over-expressed in two reports (Chen *et al.*, 2004; Ruiz *et al.*, 2012). More importantly, we found that knocking down the expression of either VLDLR or SDC2 effectively reduced collagen production, supporting the notion that these proteins play a role in the pathobiology of pulmonary fibrosis.

In conclusion, iTRAQ coupled LC-MS/MS of TGF-β1-induced fibroblasts can be utilized to identify novel markers of silica-induced lung fibrosis. Future mechanistic studies will be needed to uncover whether individual proteins are simply a marker of disease or play a biological role in the onset or progression of pulmonary fibrosis.

Ethics approval

All animal experiments were reviewed and approved by the Institutional Animal Care and Use Committee at the North China University of Science and Technology University prior to the initiation of any studies.

Consent for publication

Not applicable.

Competing interests

The authors declare that they have no competing interests.

Funding

This work was supported by the National Natural Science Foundation of China (No. 81472953); the Natural Science Foundation of Hebei Province (No. H20162091705); and Outstanding Young Foundation of North China University of Science and Technology (JP201513).

Authors' contributions

FY and HX designed the study. MN, JF, ZH, XD, YY, MN, GX, and GY carried out the experimental work, analyzed the data, and drafted the manuscript. RS participated in the design of the study and critically reviewed the manuscript and provided intellectual input. RS and RM helped write and critically reviewed the manuscript and provided intellectual input. WZ, ZB, LS, LS and WJ conceived the study, and participated in coordination, and helped in drafting the manuscript. All authors read and approved the final manuscript.

Acknowledgements

Not applicable.

REFERENCES

Agassandian, M., Tedrow, J. R., Sembrat, J., Kass, D. J., Zhang, Y., Goncharova, E. A., Kaminski, N., Mallampalli, R. K., and Vuga, L. J. (2015). VCAM-1 is a TGF-beta1 inducible gene upregulated in idiopathic pulmonary fibrosis. *Cellular signalling* **27**(12), 2467-73.

Chen, L., Klass, C., and Woods, A. (2004). Syndecan-2 regulates transforming growth factor-beta signaling. *The Journal of biological chemistry* **279**(16), 15715-8.

Eck, M. V., Oost, J., Goudriaan, J. R., Hoekstra, M., Hildebrand, R. B., Bos, I. S., van Dijk, K. W., and Van Berkel, T. J. (2005). Role of the macrophage very-low-density lipoprotein receptor in atherosclerotic lesion development. *Atherosclerosis* **183**(2), 230-7.

Gauldie, J., Sime, P. J., Xing, Z., Marr, B., and Tremblay, G. M. (1999). Transforming growth factor-beta gene transfer to the lung induces myofibroblast presence and pulmonary fibrosis. *Current topics in pathology. Ergebnisse der Pathologie* **93**, 35-45.

Harris, W. T., Kelly, D. R., Zhou, Y., Wang, D., MacEwen, M., Hagood, J. S., Clancy, J. P., Ambalavanan, N., and Sorscher, E. J. (2013). Myofibroblast differentiation and enhanced TGF-B signaling in cystic fibrosis lung disease. *PloS one* **8**(8), e70196.

Jagirdar, J., Begin, R., Dufresne, A., Goswami, S., Lee, T. C., and Rom, W. N. (1996). Transforming growth factor-beta (TGF-beta) in silicosis. *American journal of respiratory and critical care medicine* **154**(4 Pt 1), 1076-81.

Liu, Y., Xu, H., Geng, Y., Xu, D., Zhang, L., Yang, Y., Wei, Z., Zhang, B., Li, S., Gao, X., *et al.* (2017). Dibutyryl-cAMP attenuates pulmonary fibrosis by blocking myofibroblast differentiation via PKA/CREB/CBP signaling in rats with silicosis. *Respiratory research* **18**(1), 38.

Mi, H., Muruganujan, A., Casagrande, J. T., and Thomas, P. D. (2013). Large-scale gene function analysis with the PANTHER classification system. *Nature protocols* **8**(8), 1551-66.

Nesvizhskii, A. I., Keller, A., Kolker, E., and Aebersold, R. (2003). A statistical model for identifying proteins by tandem mass spectrometry. *Analytical chemistry* **75**(17), 4646-58.

Paul, D., Kumar, A., Gajbhiye, A., Santra, M. K., and Srikanth, R. (2013). Mass spectrometry-based proteomics in molecular diagnostics: discovery of cancer biomarkers using tissue culture. *BioMed research international* **2013**, 783131.

Raglow, Z., and Thomas, S. M. (2015). Tumor matrix protein collagen XIalpha1 in cancer. *Cancer*

letters **357**(2), 448-53.

Rauniyar, N., and Yates, J. R., 3rd (2014). Isobaric labeling-based relative quantification in shotgun proteomics. *Journal of proteome research* **13**(12), 5293-309.

Ruiz, X. D., Mlakar, L. R., Yamaguchi, Y., Su, Y., Larregina, A. T., Pilewski, J. M., and Feghali-Bostwick, C. A. (2012). Syndecan-2 is a novel target of insulin-like growth factor binding protein-3 and is over-expressed in fibrosis. *PloS one* **7**(8), e43049.

Seluanov, A., Vaidya, A., and Gorbunova, V. (2010). Establishing primary adult fibroblast cultures from rodents. *Journal of visualized experiments : JoVE* doi: 10.3791/2033(44).

Wisniewski, J. R., Zougman, A., Nagaraj, N., and Mann, M. (2009). Universal sample preparation method for proteome analysis. *Nature methods* **6**(5), 359-62.

Xiaojun, W., Yan, L., Hong, X., Xianghong, Z., Shifeng, L., Dingjie, X., Xuemin, G., Lijuan, Z., Bonan, Z., Zhongqiu, W., *et al.* (2016). Acetylated alpha-Tubulin Regulated by N-Acetyl-Seryl-Aspartyl-Lysyl-Proline(Ac-SDKP) Exerts the Anti-fibrotic Effect in Rat Lung Fibrosis Induced by Silica. *Scientific reports* **6**, 32257.

Xu, H., Yang, F., Sun, Y., Yuan, Y., Cheng, H., Wei, Z., Li, S., Cheng, T., Brann, D., and Wang, R. (2012). A new antifibrotic target of Ac-SDKP: inhibition of myofibroblast differentiation in rat lung with silicosis. *PloS one* **7**(7), e40301.

Table 1. Subset of differentially expressed proteins in cultured TGF-β-induced myofibroblasts relative to the untreated control

No.	Protein name	Accession Number	Molecular Weight	Fold change
1	Collagen alpha-1(II) chain	CO2A1_RAT	135 kDa	1.60
2	Cluster of Histone H2A type 1	H2A1_RAT [4]	14 kDa	1.70
3	Collagen alpha-1(V) chain	CO5A1_RAT	184 kDa	1.50
4	Protein S100-A11	S10AB_RAT	11 kDa	1.59
5	Vascular cell adhesion protein 1	VCAM1_RAT	81 kDa	1.55
6	Collagen alpha-1(XI) chain	COBA1_RAT	181 kDa	1.70
7	Cluster of Thymosin beta-4	TYB4_RAT	5 kDa	2.50
8	Cluster of Haemoglobin subunit beta-1	HBB1_RAT [2]	16 kDa	2.25
9	Haemoglobin subunit alpha-1/2	HBA_RAT	15 kDa	1.90
10	Oxidised low-density lipoprotein receptor 1	OLR1_RAT	42 kDa	1.55
11	Transmembrane protein 214	TM214_RAT	77 kDa	1.50
12	Very low-density lipoprotein receptor	VLDLR_RAT	97 kDa	1.55
13	Syndecan-2	SDC2_RAT	22 kDa	1.90
14	Serum albumin	ALBU_RAT	69 kDa	0.59
15	Histone H4	H4_RAT	11 kDa	0.25
16	Corticosteroid 11-beta-dehydrogenase isozyme 1	DHI1_RAT	32 kDa	0.65
17	Collectin-12	COL12_RAT	82 kDa	0.60
18	Cluster of Neurotrimin	NTRI_RAT [2]	38 kDa	0.65
19	Programmed cell death protein 4	PDCD4_RAT	52 kDa	0.55
20	Plasminogen receptor (KT)	PLRKT_RAT	17 kDa	0.60

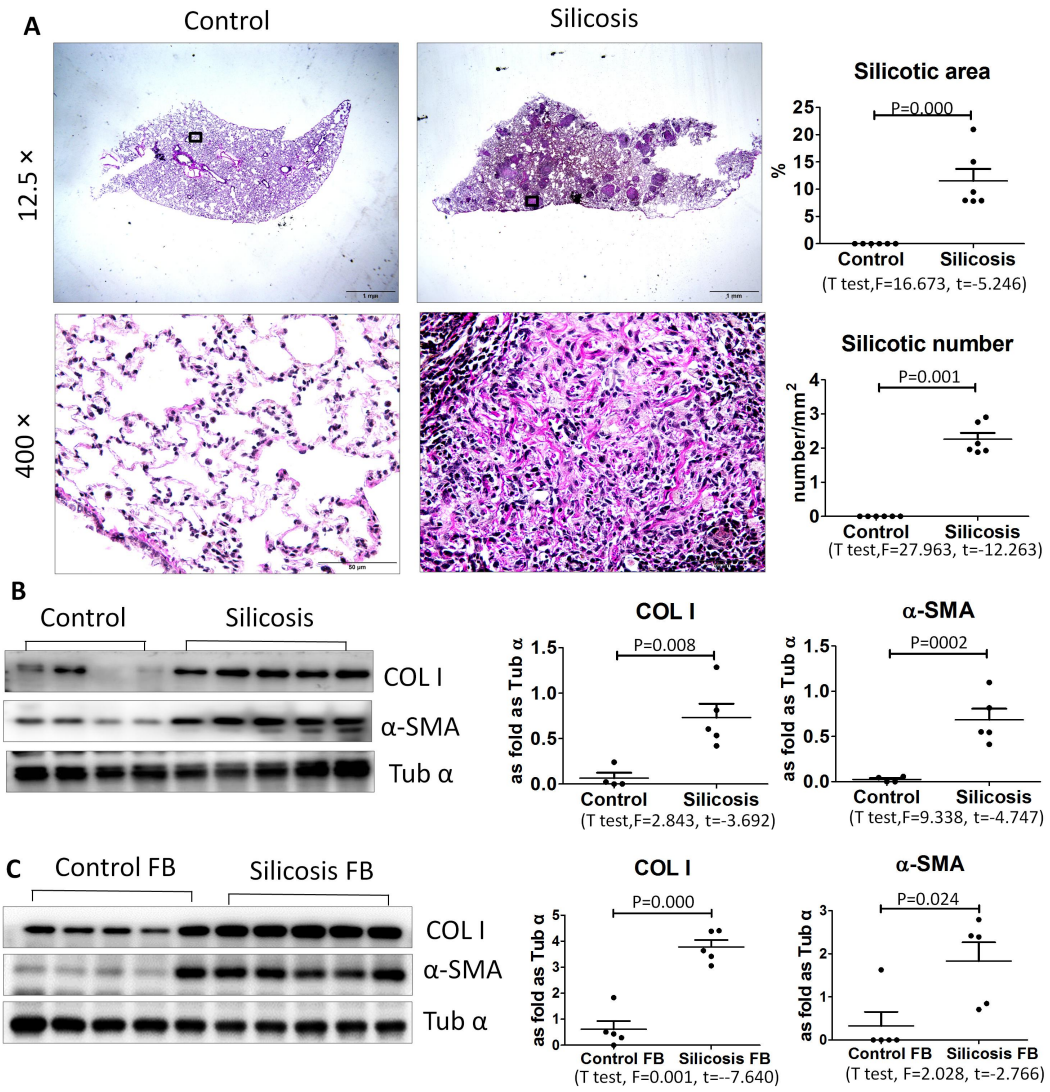

Figure 1

Figure 1.Histological examination of control and silica-exposed rat lung.A. Low (top) and high (bottom) power images of control and silica-exposed lung after van Gieson (VG) staining. Right) Quantitative assessment of area and number silicotic nodules in the lungs of control and silica-exposed rats. Western blot analysis for collagen I (COLI) and α-smooth muscle actin (α-SMA) in whole lung tissues and isolated fibroblasts from control and silica-exposed ratsAbbreviations: C, control; S, silicosis. Statistical significance was assessed using the Student's t-test.

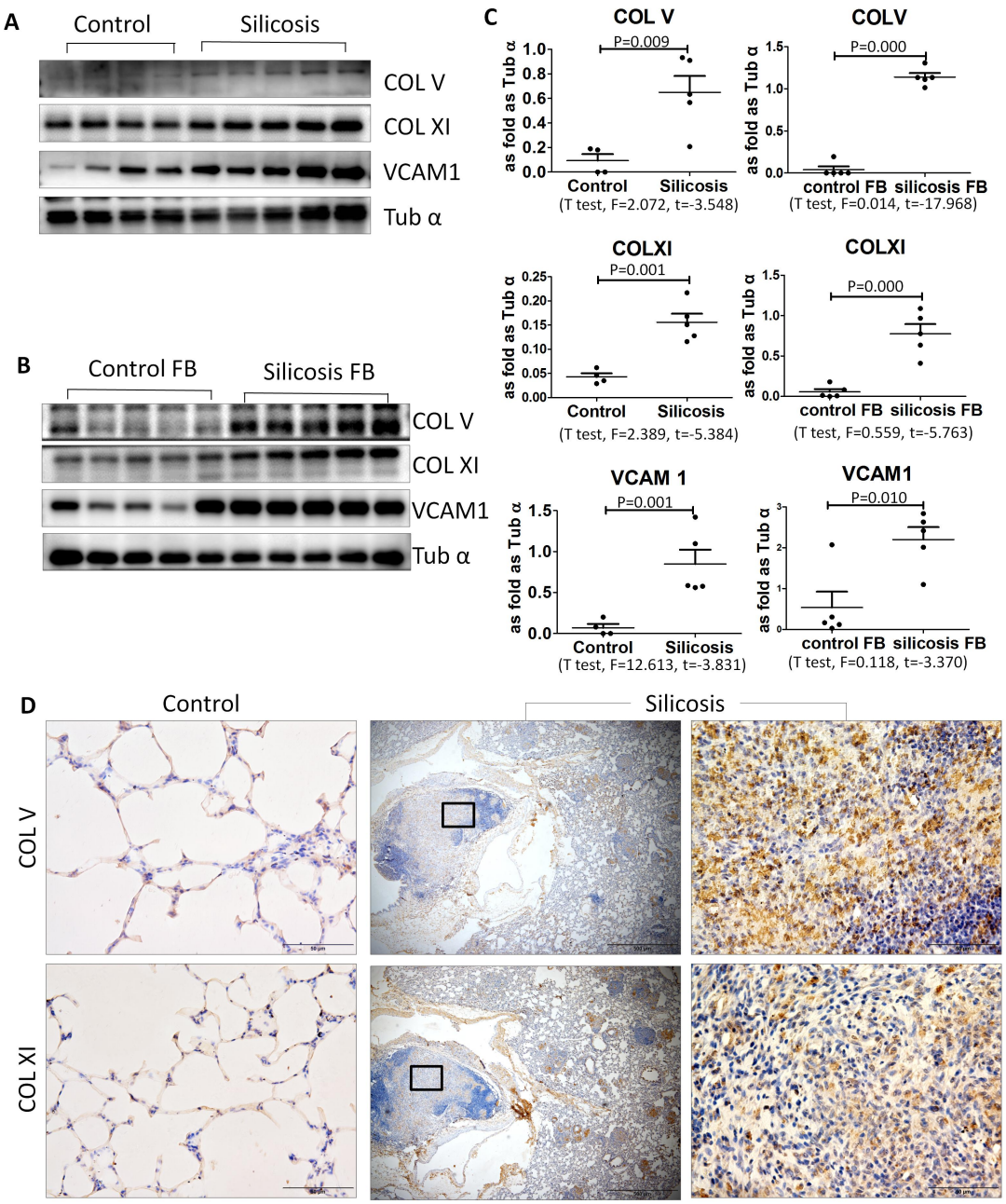

Figure 2

Figure 2. COL V, COLXI and VCAM1levels are increased in the rat lung after silicaexposure. A-C) Western blot analysis for COL V, COLXI and VCAM1 in control and silica exposed rat lung tissues. Quantitative analyses of immunoblots are shown in (C). D) IHC for expression COL V and COLXI in lung tissues from control (left) andsilica-exposed rats. Statistical significance was assessed using the Student's t-test.

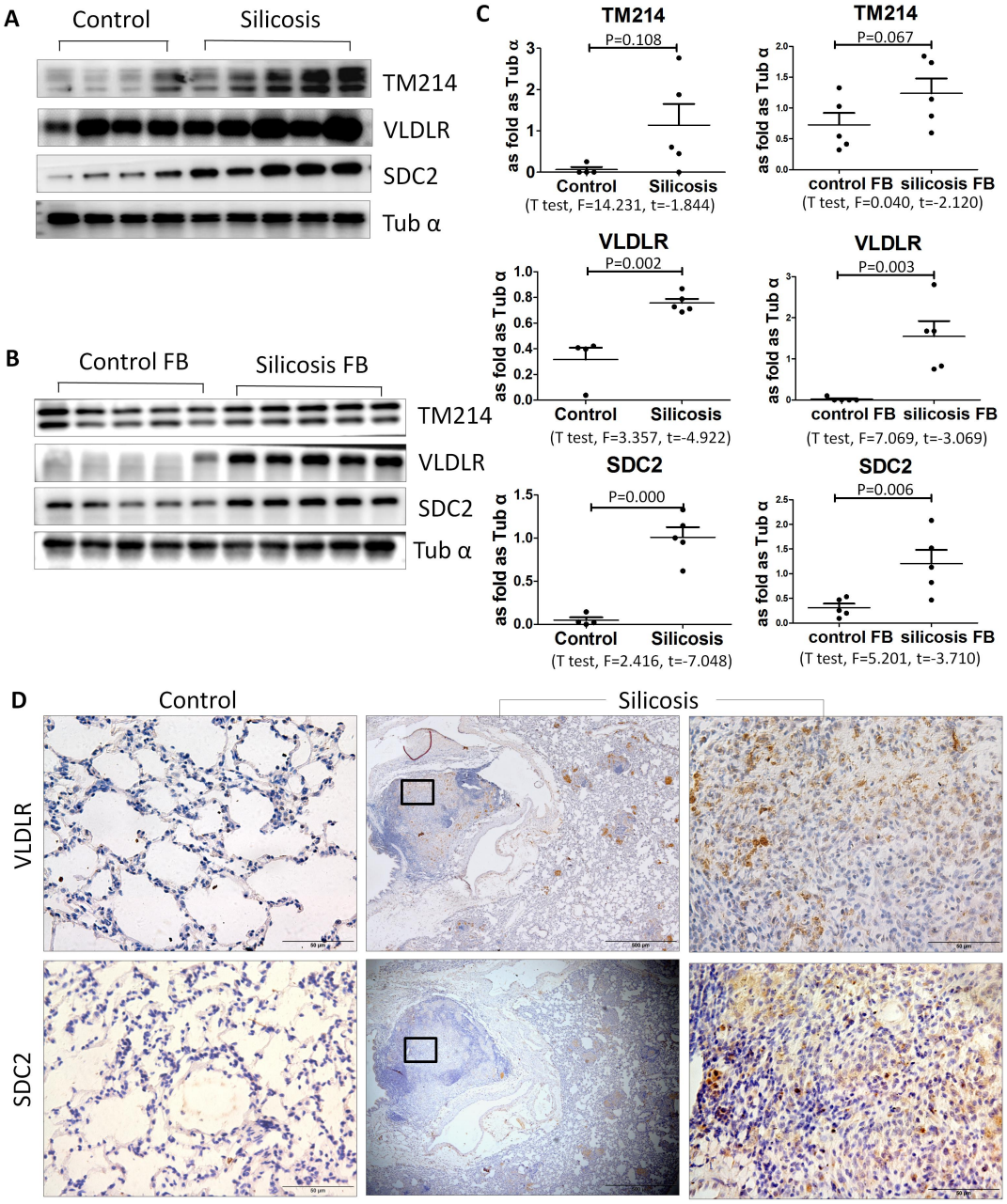

Figure 3

Figure 3.TM214, VLDLR and SDC2 expression is increased in the rat lung after silica exposure. A-C) Western blot analysis for TM214, VLDLR and SDC2 in control and silica exposed rat lung tissues. Quantitative analyses of immunoblots are shown in (C).D) IHC for expression VLDLR and SDC2 in lung tissues from control (left) andsilica-exposed rats. Statistical significance was assessed using the Student's t-test.

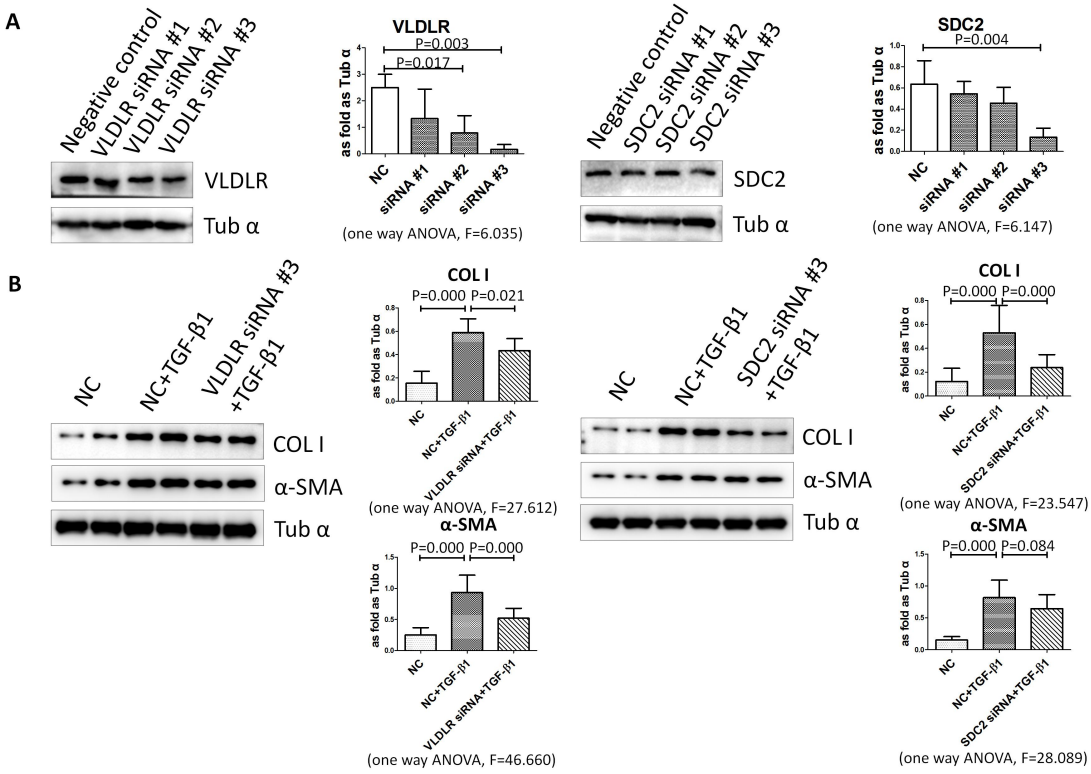

Figure 4

Figure 4. siRNA knockdown or VLDLR or SDC2 in lung fibroblasts reduces TGF-β1-induced collagen. A) Effectiveness of different siRNA probes in knockdown expression of VLDLR or SDC2. B) siRNA knockdown of VLDLR reduces expression of COL I and α-SMA in TGF-β1 treated MRC-5 fibroblasts. siRNA knockdown of SDC2 reduces expression of COL1 and causes a non-significant reduction in α-SMA in TGF-β1 treated MRC-5 fibroblasts.Statistical significance was assessed using the one way ANOVA.

Table S1 The down-regulation of differential proteins in fibroblasts induced by TGF-β1

No.	Protein Name	Accession Number	Molecular weight (Kda)	Fold
1	Histone H4 OS=Rattus norvegicus GN=Hist1h4b PE=1 SV=2	H4_RAT	11 kDa	0.25
2	Programmed cell death protein 4 OS=Rattus norvegicus GN=Pdcd4 PE=1 SV=2	PDCD4_RAT	52 kDa	0.55
3	Serum albumin OS=Rattus norvegicus GN=Alb PE=1 SV=2	ALBU_RAT	69 kDa	0.59
4	Collectin-12 OS=Rattus norvegicus GN=Colec12 PE=2 SV=1	COL12_RAT	82 kDa	0.60
5	Plasminogen receptor (KT) OS=Rattus norvegicus GN=Plgrkt PE=1 SV=1	PLRKT_RAT	17 kDa	0.60
6	Corticosteroid 11-beta-dehydrogenase isozyme 1 OS=Rattus norvegicus GN=Hsd11b1 PE=1 SV=2	DHI1_RAT	32 kDa	0.65
7	Cluster of Neurotrimin OS=Rattus norvegicus GN=Ntm PE=1 SV=1 (NTRI_RAT)	NTRI_RAT [2]	38 kDa	0.65
8	Apolipoprotein E OS=Rattus norvegicus GN=Apoe PE=1 SV=2	APOE_RAT	36 kDa	0.70
9	Galectin-3-binding protein OS=Rattus norvegicus GN=Lgals3bp PE=1 SV=2	LG3BP_RAT	64 kDa	0.70
10	Mitochondrial 2-oxoglutarate/malate carrier protein OS=Rattus norvegicus GN=Slc25a11 PE=2 SV=3	M2OM_RAT	34 kDa	0.70
11	ER membrane protein complex subunit 10 OS=Rattus norvegicus GN=Emc10 PE=1 SV=1	EMC10_RAT	27 kDa	0.70
12	Gap junction alpha-1 protein OS=Rattus norvegicus GN=Gja1 PE=1 SV=2	CXA1_RAT	43 kDa	0.70
13	Dystrobrevin beta OS=Rattus norvegicus GN=Dtnb PE=2 SV=2	DTNB_RAT	74 kDa	0.70
14	Maspardin OS=Rattus norvegicus GN=Spg21 PE=2 SV=1	SPG21_RAT	30 kDa	0.70
15	Structural maintenance of chromosomes protein 1A OS=Rattus norvegicus GN=Smc1a PE=1 SV=1	SMC1A_RAT	143 kDa	0.75
16	Phosphate carrier protein, mitochondrial OS=Rattus norvegicus GN=Slc25a3 PE=1 SV=1	MPCP_RAT	39 kDa	0.75
17	Sorting and assembly machinery component 50 homolog OS=Rattus norvegicus GN=Samm50 PE=1 SV=1	SAM50_RAT	52 kDa	0.75
18	ATP-binding cassette sub-family D member 3 OS=Rattus norvegicus GN=Abcd3 PE=1 SV=3	ABCD3_RAT	75 kDa	0.75
19	Anthrax toxin receptor 1 OS=Rattus norvegicus GN=Antxr1 PE=2 SV=2	ANTR1_RAT	62 kDa	0.75
20	Coiled-coil and C2 domain-containing protein 1A OS=Rattus norvegicus GN=Cc2d1a PE=2 SV=2	C2D1A_RAT	104 kDa	0.75
21	Proteasome activator complex subunit 2 OS=Rattus norvegicus GN=Psme2 PE=2 SV=3	PSME2_RAT	27 kDa	0.75

22	Transmembrane emp24 domain-containing protein 2 OS=Rattus norvegicus GN=Tmed2 PE=1 SV=1	TMED2_RAT	23 kDa	0.75
23	Keratin, type II cytoskeletal 4 OS=Rattus norvegicus GN=Krt4 PE=3 SV=1	K2C4_RAT	58 kDa	0.75
24	ATP synthase subunit d, mitochondrial OS=Rattus norvegicus GN=Atp5h PE=1 SV=3	ATP5H_RAT	19 kDa	0.75
25	Voltage-dependent anion-selective channel protein 3 OS=Rattus norvegicus GN=Vdac3 PE=1 SV=2	VDAC3_RAT	31 kDa	0.75
26	Ras GTPase-activating protein 1 OS=Rattus norvegicus GN=Rasa1 PE=3 SV=1	RASA1_RAT	115 kDa	0.75
27	Gamma-adducin OS=Rattus norvegicus GN=Add3 PE=1 SV=2	ADDG_RAT	79 kDa	0.75
28	Slit homolog 2 protein (Fragment) OS=Rattus norvegicus GN=Slit2 PE=1 SV=3	SLIT2_RAT	86 kDa	0.75
29	Sequestosome-1 OS=Rattus norvegicus GN=Sqstm1 PE=1 SV=1	SQSTM_RAT	48 kDa	0.75
30	Cluster of Hydroxymethylglutaryl-CoA lyase, mitochondrial OS=Rattus norvegicus GN=Hmgcl PE=2 SV=1 (HMGCL_RAT)	HMGCL_RAT	34 kDa	0.75
31	Lipid phosphate phosphohydrolase 3 OS=Rattus norvegicus GN=Ppap2b PE=1 SV=1	LPP3_RAT	35 kDa	0.75
32	39S ribosomal protein L37, mitochondrial OS=Rattus norvegicus GN=Mrpl37 PE=2 SV=1	RM37_RAT	48 kDa	0.75
33	Lipid phosphate phosphohydrolase 1 OS=Rattus norvegicus GN=Ppap2a PE=1 SV=1	LPP1_RAT	32 kDa	0.75
34	Ras-related protein Rab-13 OS=Rattus norvegicus GN=Rab13 PE=1 SV=2	RAB13_RAT	23 kDa	0.75
35	Phospholipid scramblase 3 OS=Rattus norvegicus GN=Plscr3 PE=2 SV=1	PLS3_RAT	32 kDa	0.77
36	Spectrin beta chain, non-erythrocytic 2 OS=Rattus norvegicus GN=Sptbn2 PE=1 SV=2	SPTN2_RAT	271 kDa	0.80
37	Hexokinase-1 OS=Rattus norvegicus GN=Hk1 PE=1 SV=4	HXK1_RAT	102 kDa	0.80
38	Unconventional myosin-Ib OS=Rattus norvegicus GN=Myo1b PE=1 SV=1	MYO1B_RAT	132 kDa	0.80
39	Dolichyl-diphosphooligosaccharide--protein glycosyltransferase subunit 2 OS=Rattus norvegicus GN=Rpn2 PE=2 SV=2	RPN2_RAT	69 kDa	0.80
40	Matrix Gla protein OS=Rattus norvegicus GN=Mgp PE=1 SV=2	MGP_RAT	12 kDa	0.80
41	Catalase OS=Rattus norvegicus GN=Cat PE=1 SV=3	CATA_RAT	60 kDa	0.80
42	Cluster of Caveolin-1 OS=Rattus norvegicus GN=Cav1 PE=1 SV=3 (CAV1_RAT)	CAV1_RAT	21 kDa	0.80
43	Myeloid-associated differentiation marker OS=Rattus norvegicus GN=Myadm PE=2 SV=1	MYADM_RAT	35 kDa	0.80
44	Slit homolog 3 protein OS=Rattus	SLIT3_RAT	168 kDa	0.80

	norvegicus GN=Slit3 PE=2 SV=1			
45	Voltage-dependent anion-selective channel protein 2 OS=Rattus norvegicus GN=Vdac2 PE=1 SV=2	VDAC2_RAT	32 kDa	0.80
46	Aldehyde dehydrogenase, dimeric NADP-preferring OS=Rattus norvegicus GN=Aldh3a1 PE=1 SV=3	AL3A1_RAT	50 kDa	0.80
47	Kinesin-like protein KIF1B OS=Rattus norvegicus GN=Kif1b PE=1 SV=2	KIF1B_RAT	204 kDa	0.80
48	AP2-associated protein kinase 1 OS=Rattus norvegicus GN=Aak1 PE=1 SV=1	AAK1_RAT	104 kDa	0.80
49	Serine/threonine-protein kinase MRCK alpha OS=Rattus norvegicus GN=Cdc42bpa PE=1 SV=1	MRCKA_RAT	197 kDa	0.80
50	Plexin-A3 OS=Rattus norvegicus GN=Plxna3 PE=3 SV=1	PLXA3_RAT	208 kDa	0.80
51	Keratin, type II cytoskeletal 1 OS=Rattus norvegicus GN=Krt1 PE=2 SV=1	K2C1_RAT	65 kDa	0.80
52	Calcium-binding and coiled-coil domain-containing protein 1 OS=Rattus norvegicus GN=Calcoco1 PE=2 SV=1	CACO1_RAT	77 kDa	0.80
53	Nucleolar transcription factor 1 OS=Rattus norvegicus GN=Ubtf PE=1 SV=1	UBF1_RAT	89 kDa	0.80
54	2',3'-cyclic-nucleotide 3'-phosphodiesterase OS=Rattus norvegicus GN=Cnp PE=1 SV=2	CN37_RAT	47 kDa	0.80
55	72 kDa type IV collagenase OS=Rattus norvegicus GN=Mmp2 PE=2 SV=2	MMP2_RAT	74 kDa	0.80
56	Sideroflexin-3 OS=Rattus norvegicus GN=Sfxn3 PE=2 SV=1	SFXN3_RAT	35 kDa	0.80
57	Core histone macro-H2A.1 OS=Rattus norvegicus GN=H2afy PE=1 SV=4	H2AY_RAT	40 kDa	0.80
58	5'-nucleotidase domain-containing protein 2 OS=Rattus norvegicus GN=Nt5dc2 PE=2 SV=2	NT5D2_RAT	64 kDa	0.80
59	Contactin-2 OS=Rattus norvegicus GN=Cntn2 PE=1 SV=1	CNTN2_RAT	113 kDa	0.80
60	Casein kinase II subunit alpha OS=Rattus norvegicus GN=Csnk2a1 PE=1 SV=2	CSK21_RAT	45 kDa	0.80
61	Phospholipid hydroperoxide glutathione peroxidase, nuclear OS=Rattus norvegicus GN=Gpx4 PE=2 SV=3	GPX42_RAT	29 kDa	0.80
62	Disintegrin and metalloproteinase domain-containing protein 10 (Fragment) OS=Rattus norvegicus GN=Adam10 PE=2 SV=1	ADA10_RAT	60 kDa	0.80
63	Alpha-adducin OS=Rattus norvegicus GN=Add1 PE=2 SV=2	ADDA_RAT	80 kDa	0.80
64	Mitochondrial carnitine/acylcarnitine carrier protein OS=Rattus norvegicus GN=Slc25a20 PE=1 SV=1	MCAT_RAT	33 kDa	0.80
65	Basic leucine zipper and W2 domain-containing protein 2 OS=Rattus norvegicus GN=Bzw2 PE=2 SV=1	BZW2_RAT	48 kDa	0.80
66	Protein Wnt-5a OS=Rattus norvegicus GN=Wnt5a PE=2 SV=2	WNT5A_RAT	42 kDa	0.80
67	Phosphatidylinositol 3-kinase regulatory	P85A_RAT	84 kDa	0.80

	subunit alpha OS=Rattus norvegicus GN=Pik3r1 PE=1 SV=1			
68	Microtubule-associated protein RP/EB family member 2 OS=Rattus norvegicus GN=Mapre2 PE=2 SV=1	MARE2_RAT	37 kDa	0.80
69	ADP-ribosyl cyclase/cyclic ADP-ribose hydrolase 2 OS=Rattus norvegicus GN=Bst1 PE=2 SV=1	BST1_RAT	35 kDa	0.80
70	Insulin-like growth factor-binding protein 5 OS=Rattus norvegicus GN=Igfbp5 PE=1 SV=1	IBP5_RAT	30 kDa	0.80
71	Trophoblast glycoprotein OS=Rattus norvegicus GN=Tpbg PE=2 SV=1	TPBG_RAT	47 kDa	0.80
72	Tubulin-specific chaperone E OS=Rattus norvegicus GN=Tbce PE=2 SV=1	TBCE_RAT	59 kDa	0.80
73	3-mercaptopyruvate sulfurtransferase OS=Rattus norvegicus GN=Mpst PE=1 SV=3	THTM_RAT	33 kDa	0.80
74	DnaJ homolog subfamily B member 6 OS=Rattus norvegicus GN=Dnajb6 PE=1 SV=1	DNJB6_RAT	39 kDa	0.80
75	Hydroxyacylglutathione hydrolase, mitochondrial OS=Rattus norvegicus GN=Hagh PE=1 SV=2	GLO2_RAT	34 kDa	0.80
76	Cathepsin L1 OS=Rattus norvegicus GN=Ctsl PE=1 SV=2	CATL1_RAT	38 kDa	0.80
77	Magnesium transporter protein 1 OS=Rattus norvegicus GN=Magt1 PE=2 SV=2	MAGT1_RAT	38 kDa	0.80
78	Collagen triple helix repeat-containing protein 1 OS=Rattus norvegicus GN=Cthrc1 PE=1 SV=1	CTHR1_RAT	26 kDa	0.80
79	Methylosome protein 50 OS=Rattus norvegicus GN=Wdr77 PE=1 SV=1	MEP50_RAT	37 kDa	0.80
80	Transmembrane 7 superfamily member 3 OS=Rattus norvegicus GN=Tm7sf3 PE=2 SV=1	TM7S3_RAT	64 kDa	0.80
81	Cytochrome c oxidase subunit 7C, mitochondrial OS=Rattus norvegicus GN=Cox7c PE=1 SV=2	COX7C_RAT	7 kDa	0.80

Table S2 The up-regulation of differential proteins in fibroblasts induced by TGF-β1

No.	Protein Name	Accession Number	Molecular weight (Kda)	Fold
1	Cluster of Thymosin beta-4 OS=Rattus norvegicus GN=Tmsb4x PE=2 SV=2 (TYB4_RAT)	TYB4_RAT	5 kDa	2.50
2	Cluster of Hemoglobin subunit beta-1 OS=Rattus norvegicus GN=Hbb PE=1 SV=3 (HBB1_RAT)	HBB1_RAT [2]	16 kDa	2.25
3	Hemoglobin subunit alpha-1/2 OS=Rattus norvegicus GN=Hba1 PE=1 SV=3	HBA_RAT	15 kDa	1.90
4	Syndecan-2 OS=Rattus norvegicus GN=Sdc2 PE=2 SV=2	SDC2_RAT	22 kDa	1.90
5	Cluster of Histone H2A type 1 OS=Rattus norvegicus PE=1 SV=2 (H2A1_RAT)	H2A1_RAT [4]	14 kDa	1.70
6	Collagen alpha-1(XI) chain OS=Rattus norvegicus GN=Col11a1 PE=1 SV=2	COBA1_RAT	181 kDa	1.70
7	Collagen alpha-1(II) chain OS=Rattus norvegicus GN=Col2a1 PE=1 SV=2	CO2A1_RAT	135 kDa	1.60
8	Protein S100-A11 OS=Rattus norvegicus GN=S100a11 PE=3 SV=1	S10AB_RAT	11 kDa	1.59
9	Vascular cell adhesion protein 1 OS=Rattus norvegicus GN=Vcam1 PE=2 SV=1	VCAM1_RAT	81 kDa	1.55
10	Oxidized low-density lipoprotein receptor 1 OS=Rattus norvegicus GN=Olr1 PE=2 SV=1	OLR1_RAT	42 kDa	1.55
11	Very low-density lipoprotein receptor OS=Rattus norvegicus GN=Vldlr PE=2 SV=1	VLDLR_RAT	97 kDa	1.55
12	Collagen alpha-1(V) chain OS=Rattus norvegicus GN=Col5a1 PE=1 SV=1	CO5A1_RAT	184 kDa	1.50
13	Transmembrane protein 214 OS=Rattus norvegicus GN=Tmem214 PE=2 SV=1	TM214_RAT	77 kDa	1.50
14	Protein-lysine 6-oxidase OS=Rattus norvegicus GN=Lox PE=1 SV=2	LYOX_RAT	47 kDa	1.45
15	ATPase inhibitor, mitochondrial OS=Rattus norvegicus GN=Atpif1 PE=3 SV=2	ATIF1_RAT	12 kDa	1.40
16	Collagen alpha-1(III) chain OS=Rattus norvegicus GN=Col3a1 PE=2 SV=3	CO3A1_RAT	139 kDa	1.35
17	Tropomyosin beta chain OS=Rattus norvegicus GN=Tpm2 PE=3 SV=1	TPM2_RAT	33 kDa	1.35
18	60S ribosomal protein L26 OS=Rattus norvegicus GN=Rpl26 PE=1 SV=1	RL26_RAT	17 kDa	1.35
19	Protein PRRC1 OS=Rattus norvegicus GN=Prrc1 PE=2 SV=1	PRRC1_RAT	46 kDa	1.35

20	S-adenosylmethionine synthase isoform type-2 OS=Rattus norvegicus GN=Mat2a PE=1 SV=1	METK2_RAT	44 kDa	1.35
21	Synaptobrevin homolog YKT6 OS=Rattus norvegicus GN=Ykt6 PE=1 SV=1	YKT6_RAT	22 kDa	1.35
22	60S ribosomal protein L37a OS=Rattus norvegicus GN=Rpl37a PE=1 SV=1	RL37A_RAT	8 kDa	1.35
23	Solute carrier family 2, facilitated glucose transporter member 1 OS=Rattus norvegicus GN=Slc2a1 PE=1 SV=1	GTR1_RAT	54 kDa	1.35
24	Pulmonary surfactant-associated protein A OS=Rattus norvegicus GN=Sftpa1 PE=1 SV=3	SFTPA_RAT	26 kDa	1.35
25	Small ubiquitin-related modifier 2 OS=Rattus norvegicus GN=Sumo2 PE=1 SV=1	SUMO2_RAT	11 kDa	1.35
26	E3 ubiquitin-protein ligase RNF181 OS=Rattus norvegicus GN=Rnf181 PE=1 SV=1	RN181_RAT	19 kDa	1.35
27	Collagen alpha-1(I) chain OS=Rattus norvegicus GN=Col1a1 PE=1 SV=5	CO1A1_RAT	138 kDa	1.30
28	E3 ubiquitin-protein ligase PDZRN3 OS=Rattus norvegicus GN=Pdzrn3 PE=1 SV=1	PZRN3_RAT	119 kDa	1.30
29	60S ribosomal protein L23a OS=Rattus norvegicus GN=Rpl23a PE=2 SV=1	RL23A_RAT	18 kDa	1.30
30	40S ribosomal protein S19 OS=Rattus norvegicus GN=Rps19 PE=2 SV=3	RS19_RAT	16 kDa	1.30
31	Translation initiation factor eIF-2B subunit gamma OS=Rattus norvegicus GN=Eif2b3 PE=2 SV=2	EI2BG_RAT	50 kDa	1.30
32	Protein phosphatase inhibitor 2 OS=Rattus norvegicus GN=Ppp1r2 PE=2 SV=2	IPP2_RAT	23 kDa	1.30
33	PHD finger-like domain-containing protein 5A OS=Rattus norvegicus GN=Phf5a PE=2 SV=1	PHF5A_RAT	12 kDa	1.30
34	Ras-related protein Rab-27A OS=Rattus norvegicus GN=Rab27a PE=1 SV=1	RB27A_RAT	25 kDa	1.30
35	Fibroblast growth factor 2 OS=Rattus norvegicus GN=Fgf2 PE=2 SV=1	FGF2_RAT	17 kDa	1.30
36	Proteinase-activated receptor 1 OS=Rattus norvegicus GN=F2r PE=2 SV=1	PAR1_RAT	48 kDa	1.30
37	Collagen alpha-2(I) chain OS=Rattus norvegicus GN=Col1a2 PE=1 SV=3	CO1A2_RAT	130 kDa	1.25
38	Procollagen-lysine,2-oxoglutarate	PLOD2_RAT	85 kDa	1.25

	5-dioxygenase 2 OS=Rattus norvegicus GN=Plod2 PE=2 SV=1			
39	40S ribosomal protein S13 OS=Rattus norvegicus GN=Rps13 PE=1 SV=2	RS13_RAT	17 kDa	1.25
40	Plasminogen activator inhibitor 1 OS=Rattus norvegicus GN=Serpine1 PE=2 SV=1	PAI1_RAT	45 kDa	1.25
41	Membrane-associated guanylate kinase, WW and PDZ domain-containing protein 3 OS=Rattus norvegicus GN=Magi3 PE=1 SV=2	MAGI3_RAT	161 kDa	1.25
42	Plasminogen activator inhibitor 1 RNA-binding protein OS=Rattus norvegicus GN=Serbp1 PE=1 SV=2	PAIRB_RAT	45 kDa	1.25
43	Translationally-controlled tumor protein OS=Rattus norvegicus GN=Tpt1 PE=1 SV=1	TCTP_RAT	19 kDa	1.25
44	Nucleolar and coiled-body phosphoprotein 1 OS=Rattus norvegicus GN=Nolc1 PE=1 SV=1	NOLC1_RAT	74 kDa	1.25
45	60S ribosomal protein L35a OS=Rattus norvegicus GN=Rpl35a PE=3 SV=1	RL35A_RAT	13 kDa	1.25
46	Oligoribonuclease, mitochondrial OS=Rattus norvegicus GN=Rexo2 PE=2 SV=1	ORN_RAT	27 kDa	1.25
47	Protein CYR61 OS=Rattus norvegicus GN=Cyr61 PE=2 SV=1	CYR61_RAT	42 kDa	1.25
48	Protein TANC1 OS=Rattus norvegicus GN=Tanc1 PE=1 SV=1	TANC1_RAT	201 kDa	1.25
49	Guanine nucleotide-binding protein-like 3 OS=Rattus norvegicus GN=Gnl3 PE=1 SV=1	GNL3_RAT	61 kDa	1.25
50	Glutamine--fructose-6-phosphate aminotransferase [isomerizing] 2 OS=Rattus norvegicus GN=Gfpt2 PE=2 SV=3	GFPT2_RAT	77 kDa	1.25
51	Osteopontin OS=Rattus norvegicus GN=Spp1 PE=1 SV=2	OSTP_RAT	35 kDa	1.25
52	60S ribosomal protein L36a OS=Rattus norvegicus GN=Rpl36a PE=1 SV=2	RL36A_RAT	12 kDa	1.25
53	CDK5 regulatory subunit-associated protein 3 OS=Rattus norvegicus GN=Cdk5rap3 PE=1 SV=1	CK5P3_RAT	57 kDa	1.25
54	40S ribosomal protein S25 OS=Rattus norvegicus GN=Rps25 PE=2 SV=1	RS25_RAT	14 kDa	1.25
55	Growth factor receptor-bound protein 10 OS=Rattus norvegicus GN=Grb10 PE=3 SV=1	GRB10_RAT	68 kDa	1.25
56	ADP-ribosylation factor GTPase-activating	ARFG1_RAT	45 kDa	1.25

	protein 1 OS=Rattus norvegicus GN=Arfgap1 PE=1 SV=1			
57	Squalene synthase OS=Rattus norvegicus GN=Fdft1 PE=2 SV=1	FDFT_RAT	48 kDa	1.25
58	Striatin-3 OS=Rattus norvegicus GN=Strn3 PE=2 SV=2	STRN3_RAT	87 kDa	1.25
59	Squalene monooxygenase OS=Rattus norvegicus GN=Sqle PE=2 SV=1	ERG1_RAT	64 kDa	1.25
60	Calcium-regulated heat stable protein 1 OS=Rattus norvegicus GN=Carhsp1 PE=1 SV=1	CHSP1_RAT	16 kDa	1.25
61	Rho guanine nucleotide exchange factor 6 OS=Rattus norvegicus GN=Arhgef6 PE=2 SV=1	ARHG6_RAT	87 kDa	1.25
62	DnaJ homolog subfamily C member 25 OS=Rattus norvegicus GN=Dnajc25 PE=2 SV=1	DJC25_RAT	42 kDa	1.25
63	ER membrane protein complex subunit 8 OS=Rattus norvegicus GN=Emc8 PE=2 SV=1	EMC8_RAT	23 kDa	1.25
64	Glutamate--cysteine ligase regulatory subunit OS=Rattus norvegicus GN=Gclm PE=1 SV=1	GSH0_RAT	31 kDa	1.25
65	Small ubiquitin-related modifier 3 OS=Rattus norvegicus GN=Sumo3 PE=3 SV=1	SUMO3_RAT	12 kDa	1.25
66	Leucine-rich repeat flightless-interacting protein 1 OS=Rattus norvegicus GN=Lrrfip1 PE=1 SV=1	LRRF1_RAT	80 kDa	1.20
67	40S ribosomal protein S12 OS=Rattus norvegicus GN=Rps12 PE=1 SV=2	RS12_RAT	15 kDa	1.20
68	Serine/threonine-protein phosphatase 2A 65 kDa regulatory subunit A beta isoform OS=Rattus norvegicus GN=Ppp2r1b PE=2 SV=1	2AAB_RAT	66 kDa	1.20
69	Acyl-protein thioesterase 2 OS=Rattus norvegicus GN=Lypla2 PE=1 SV=1	LYPA2_RAT	25 kDa	1.20
70	Phosducin-like protein 3 OS=Rattus norvegicus GN=Pdcl3 PE=2 SV=1	PDCL3_RAT	28 kDa	1.20
71	Dihydrofolate reductase OS=Rattus norvegicus GN=Dhfr PE=2 SV=3	DYR_RAT	22 kDa	1.20
72	Alkyldihydroxyacetonephosphate synthase, peroxisomal OS=Rattus norvegicus GN=Agps PE=2 SV=1	ADAS_RAT	72 kDa	1.20
73	Arylsulfatase B OS=Rattus norvegicus	ARSB_RAT	59 kDa	1.20

	GN=Arsb PE=2 SV=2			
74	60S ribosomal protein L36 OS=Rattus norvegicus GN=Rpl36 PE=1 SV=2	RL36_RAT	12 kDa	1.20
75	Malignant T-cell-amplified sequence 1 OS=Rattus norvegicus GN=Mcts1 PE=2 SV=1	MCTS1_RAT	21 kDa	1.20
76	Calcium-binding mitochondrial carrier protein SCaMC-2 OS=Rattus norvegicus GN=Slc25a25 PE=1 SV=1	SCMC2_RAT	53 kDa	1.20
77	V-type proton ATPase subunit F OS=Rattus norvegicus GN=Atp6v1f PE=1 SV=1	VATF_RAT	13 kDa	1.20
78	PEST proteolytic signal-containing nuclear protein OS=Rattus norvegicus GN=Pcnp PE=2 SV=1	PCNP_RAT	20 kDa	1.20
79	Protein disulfide-isomerase OS=Rattus norvegicus GN=P4hb PE=1 SV=2	PDIA1_RAT	57 kDa	1.20
80	78 kDa glucose-regulated protein OS=Rattus norvegicus GN=Hspa5 PE=1 SV=1	GRP78_RAT	72 kDa	1.20
81	40S ribosomal protein S3a OS=Rattus norvegicus GN=Rps3a PE=1 SV=2	RS3A_RAT	30 kDa	1.20
82	Custer of Ras-related protein Rab-1A OS=Rattus norvegicus GN=Rab1A PE=1 SV=3 (RAB1A_RAT)	RAB1A_RAT [2]	23 kDa	1.20
83	Farnesyl pyrophosphate synthase OS=Rattus norvegicus GN=Fdps PE=2 SV=2	FPPS_RAT	41 kDa	1.20
84	40S ribosomal protein S16 OS=Rattus norvegicus GN=Rps16 PE=1 SV=2	RS16_RAT	16 kDa	1.20
85	40S ribosomal protein S18 OS=Rattus norvegicus GN=Rps18 PE=1 SV=3	RS18_RAT	18 kDa	1.20
86	40S ribosomal protein S11 OS=Rattus norvegicus GN=Rps11 PE=1 SV=3	RS11_RAT	18 kDa	1.20
87	Transforming protein RhoA OS=Rattus norvegicus GN=Rhoa PE=1 SV=1	RHOA_RAT	22 kDa	1.20
88	Tubulin-specific chaperone A OS=Rattus norvegicus GN=Tbca PE=1 SV=1	TBCA_RAT	13 kDa	1.20
89	Transcriptional activator protein Pur-beta OS=Rattus norvegicus GN=Purb PE=1 SV=3	PURB_RAT	33 kDa	1.20
90	60S ribosomal protein L10a OS=Rattus norvegicus GN=Rpl10a PE=1 SV=2	RL10A_RAT	25 kDa	1.20
91	60S ribosomal protein L11 OS=Rattus norvegicus GN=Rpl11 PE=1 SV=2	RL11_RAT	20 kDa	1.20
92	40S ribosomal protein S20 OS=Rattus norvegicus GN=Rps20 PE=3 SV=1	RS20_RAT	13 kDa	1.20
93	Procollagen C-endopeptidase enhancer 1	PCOC1_RAT	50 kDa	1.20

	OS=Rattus norvegicus GN=Pcolce PE=1 SV=1			
94	60S ribosomal protein L17 OS=Rattus norvegicus GN=Rpl17 PE=2 SV=3	RL17_RAT	21 kDa	1.20
95	Phosphatidylinositol-binding clathrin assembly protein OS=Rattus norvegicus GN=Picalm PE=1 SV=1	PICAL_RAT	69 kDa	1.20
96	Translocon-associated protein subunit alpha OS=Rattus norvegicus GN=Ssr1 PE=2 SV=1	SSRA_RAT	36 kDa	1.20
97	Protein FAM98A OS=Rattus norvegicus GN=Fam98a PE=2 SV=1	FA98A_RAT	55 kDa	1.20
98	Follistatin-related protein 1 OS=Rattus norvegicus GN=Fstl1 PE=1 SV=1	FSTL1_RAT	35 kDa	1.20
99	Cytosolic phospholipase A2 OS=Rattus norvegicus GN=Pla2g4a PE=2 SV=1	PA24A_RAT	86 kDa	1.20
100	Protein phosphatase methylesterase 1 OS=Rattus norvegicus GN=Ppme1 PE=1 SV=2	PPME1_RAT	42 kDa	1.20
101	Cysteine-rich protein 2 OS=Rattus norvegicus GN=Crip2 PE=2 SV=1	CRIP2_RAT	23 kDa	1.20
102	40S ribosomal protein S17 OS=Rattus norvegicus GN=Rps17 PE=1 SV=3	RS17_RAT	16 kDa	1.20
103	Phosphoserine phosphatase OS=Rattus norvegicus GN=Psph PE=2 SV=1	SERB_RAT	25 kDa	1.20
104	Cystathionine gamma-lyase OS=Rattus norvegicus GN=Cth PE=1 SV=2	CGL_RAT	44 kDa	1.20
105	Glia maturation factor beta OS=Rattus norvegicus GN=Gmfb PE=1 SV=2	GMFB_RAT	17 kDa	1.20
106	Prothrombin OS=Rattus norvegicus GN=F2 PE=1 SV=1	THRB_RAT	70 kDa	1.20
107	Calcyclin-binding protein OS=Rattus norvegicus GN=Cacybp PE=1 SV=1	CYBP_RAT	27 kDa	1.20
108	3-hydroxyisobutyryl-CoA hydrolase, mitochondrial OS=Rattus norvegicus GN=Hibch PE=1 SV=2	HIBCH_RAT	43 kDa	1.20
109	40S ribosomal protein S24 OS=Rattus norvegicus GN=Rps24 PE=2 SV=1	RS24_RAT	15 kDa	1.20
110	Pyridoxal kinase OS=Rattus norvegicus GN=Pdxk PE=1 SV=1	PDXK_RAT	35 kDa	1.20
111	Sodium/potassium-transporting ATPase subunit beta-1 OS=Rattus norvegicus GN=Atp1b1 PE=1 SV=1	AT1B1_RAT	35 kDa	1.20
112	ER membrane protein complex subunit 3 OS=Rattus norvegicus GN=Emc3 PE=2	EMC3_RAT	30 kDa	1.20

	SV=3			
113	40S ribosomal protein S28 OS=Rattus norvegicus GN=Rps28 PE=1 SV=1	RS28_RAT	8 kDa	1.20
114	Cell growth regulator with EF hand domain protein 1 OS=Rattus norvegicus GN=Cgref1 PE=1 SV=1	CGRE1_RAT	31 kDa	1.20
115	40S ribosomal protein S27 OS=Rattus norvegicus GN=Rps27 PE=2 SV=3	RS27_RAT	9 kDa	1.20

Table S3. GO analysis of differential proteins performed in PANTHER and classified based on molecular function

molecular function	Up-regulated proteins		Down-regulated proteins	
catalytic activity (GO:0003824)	37	PDCL3; LYOX; TANC1; GMFB; CGL; FPPS; VATF; PDIA1; PCOC1; PPME1; ARHG6; LYPA2; SERB; TPM2; PDXK; ARSB; ERG1; ORN; EI2BG; RHOA; HIBCH; CK5P3; 2AAB; METK2; GFPT2; DYR; THRB; MAGI3; PAI1; PA24A; CYBP; ARFG1; ADAS; ATIF1; IPP2; GSH0; GNL3	28	KIF1B; SMC1A; THTM; MRCKA; CAV1; BST1; CATL1; AL3A1; CATA; RPN2; CN37; CTHR1; LPP3; DHI1; PSME2; RASA1; COX7C; LPP1; P85A; GLO2; MAGT1; AAK1; BZW2; APOE; MYO1B; HXK1; NT5D2; HMGCL
binding (GO:0005488)	24	GMFB; FGF2; CRIP2; SSRA; PCOC1; PAIRB; ARHG6; RL10A; S10AB; SERB; PURB; EI2BG; LRRF1; RHOA; FSTL1; CYR61; OLR1; TCTP; ARFG1; CHSP1; RS13; ATIF1; RL35A; YKT6	18	SMC1A; CAV1; CATA; ADDG; MARE2; DTNB; H2AY; SQSTM; P85A; SPTN2; IBP5; AAK1; ADDA; C2D1A; APOE; H4; MYO1B; WNT5A
structural molecule activity (GO:0005198)	19	RL11; RS11; CRIP2; RS20; RS12; RS28; RS16; RL10A; RS27; SCMC2; TPM2; RS18; RL23A; RL36; RL26; RS19; TCTP; RS13; RL35A	14	CAV1; M2OM; K2C1; ADDG; MGP; COL12; MARE2; DTNB; K2C4; MCAT; SPTN2; ADDA; MYO1B; MPCP
transporter activity (GO:0005215)	4	CGRE1; VATF; PCOC1; AT1B1	7	VDAC2; PLS3; SFXN3; VDAC3; ABCD3; APOE; CXA1
receptor activity (GO:0004872)	3	LYOX; PCOC1; MCTS1	4	NTRI; ANTR1; MEP50; TPBG
translation regulator activity (GO:0045182)	1	EI2BG	2	PDCD4; BZW2
antioxidant activity	0		1	CATA

Table S4. GO analysis of differential proteins performed in PANTHER and classified based on biological process

biological process		Up-regulation proteins		Down-regulation proteins
cellular process (GO:0009987)	51	GNL3; RL11; LYOX; RS11; RB27A; FPPS; FGF2; VATF; PDIA1; PCOC1; PZRN3; RS28; ARHG6; ARHG6; RS16; LYPA2; RS16; LYPA2; GRB10; RS27; S10AB; SERB; SCMC2; RS17; TPM2; RAB1A; RS18; RL23A; PDXK; SUMO2; ORN; RL36; RHOA; RL26; GFPT2; CYR61; MCTS1; MAGI3; RS19; SDC2; OLR1; ARFG1; CHSP1; PHF5A; RS13; ATIF1; SUMO3; RN181; IPP2; RL35A; YKT6; EMC3; GSH0; GNL3	42	TBCE; KIF1B; SMC1A; MRCKA; CAV1; M2OM; BST1; CATL1; PLS3; NTRI; CATA; SLIT3; K2C1; RPN2; CTHR1; LPP3; COL12; MARE2; DTNB; H2AY; K2C4; SQSTM; RASA1; LPP1; MEP50; MCAT; SPTN2; IBP5; TPBG; AAK1; C2D1A; APOE; H4; MYO1B; HXK1; CXA1; MPCP; NT5D2; SLIT2; WNT5A; PLXA3
metabolic process (GO:0008152)	50	PDCL3; RL11; LYOX; RS11; CGL; FPPS; CRIP2; TBCA; VATF; SSRA; PCOC1; PAIRB; PPME1; RS16; RL10A; LYPA2; RS27; S10AB; SERB; SCMC2; PURB; RS17; RS18; RL23A; PDXK; SUMO2; ARSB; ORN; EI2BG; RL36; LRRF1; HIBCH; CK5P3; RL26; GFPT2; THRB; PA24A; CYBP; CHSP1; PHF5A; ADAS; RS13; ATIF1; SUMO3; RN181; IPP2; RL35A; EMC3; GSH0; GNL3	29	KIF1B; SMC1A; THTM; CAV1; M2OM; CATL1; CATA; RPN2; LPP3; DHI1; H2AY; PSME2; SQSTM; RASA1; ABCD3; COX7C; LPP1; MEP50; P85A; MCAT;
cellular component organization or biogenesis (GO:0071840)	16	RL11; CRIP2; PZRN3; RS28; RS16; RS27; RS17; TPM2; RS18; RL23A; RL23A; RL26; RS19; SDC2; RL35A; YKT6; GNL3	20	TBCE; SMC1A; PLS3; SLIT3; K2C1; ADDG; CTHR1; COL12; MARE2; DTNB; H2AY; K2C4; MEP50; AAK1; ADDA; APOE; H4; MYO1B; SLIT2; PLXA3;
multicellular organismal process	15	CO2A1; PCOC1; PZRN3; ARHG6; COBA1; TPM2; CO3A1; SFTPA; MAGI3; HBB1; CO5A1; SDC2; HBA; CO1A1; CO1A2	7	SLIT3; ADA10; APOE; MYO1B; SLIT2; WNT5A; PLXA3

(GO:0032501)				
localization (GO:0051179)	14	LYOX; RB27A; PICAL; CGRE1; VATF; SSRA; PCOC1; RS28; RAB1A; RHOA; HBB1; SDC2; YKT6; HBA	14	KIF1B; THTM; CAV1; VDAC2; PLS3; ALBU; TMED2; VDAC3; ABCD3; MEP50; AAK1; APOE; MYO1B; PLXA3
developmental process (GO:0032502)	13	CO2A1; GMFB; FGF2; CRIP2; PDIA1; PCOC1; PZRN3; COBA1; TPM2; CYR61; SDC2; CO1A2	12	MRCKA; NTRI; SLIT3; PDCD4; ADA10; COL12; SPTN2; APOE; MYO1B; SLIT2; WNT5A; PLXA3
immune system process (GO:0002376)	12	LYOX; CRIP2; PCOC1; ARHG6; COBA1; S10AB; CO3A1; SFTPA; CO5A1; PA24A; OLR1; CO1A1	4	BST1; COL12; PSME2; GLO2
biological regulation (GO:0065007)	9	LYOX; RB27A; CRIP2; PDIA1; CK5P3; SFTPA; CYR61; PAI1; GSH0	14	BST1; PLS3; LPP3; H2AY; PSME2; SQSTM; LPP1; IBP5; AAK1; APOE; HXK1; SLIT2; WNT5A; PLXA3
response to stimulus (GO:0050896)	7	CGRE1; CRIP2; PDIA1; PCOC1; ARHG6; CYR61; THRB	15	THTM; CATA; LPP3; PSME2; SQSTM; RASA1; LPP1; P85A; GLO2; IBP5; AAK1; APOE; SLIT2; WNT5A; PLXA3
biological adhesion (GO:0022610)	4	LYOX; PCOC1; PLOD2; CYR61	2	CTHR1; COL12
locomotion (GO:0040011)	1	SDC2	2	SLIT2; PLXA3
reproduction (GO:0000003)	1	CRIP2	1	ADA10

Table S5. GO analysis of differential proteins performed in PANTHER and classified based on cellular component

cellular component	Up-regulation proteins		Down-regulation proteins	
cell part (GO:0044464)	43	PDCL3; RL11; RS11; RB27A; PICAL; FPPS; CRIP2; RS20; RS12; NOLC1; RS28; RS16; FA98A; FA98A; LYPA2; RS27; SERB; RS17; TPM2; RAB1A; RS18; RL36A; RL23A; PDXK; SUMO2; RL36; CK5P3; RL26; METK2; RS19; SDC2; PA24A; TCTP; PHF5A; RS13; ATIF1; SUMO3; IPP2; RL35A; YKT6; EMC3; GSH0; RS3A; GNL3	23	KIF1B; CATL1; CATA; K2C1; RPN2; RM37; ADDG; CN37; MARE2; DTNB; TMED2; H2AY; K2C4; PSME2; SQSTM; RASA1; P85A; SPTN2; AAK1; ADDA; C2D1A; MYO1B; HXK1
organelle (GO:0043226)	26	RL11; RS11; RB27A; RS20; RS12; NOLC1; RS28; RS16; RS27; RS17; RAB1A; RS18; RL36A; RL23A; SUMO2; RL36; RL26; RS19; TCTP; PHF5A; RS13; ATIF1; SUMO3; RL35A; EMC3; GNL3	15	KIF1B; CATL1; K2C1; RPN2; RM37; ADDG; MARE2; DTNB; H2AY; K2C4; PSME2; SQSTM; ADDA; C2D1A; MYO1B
macromolecular complex (GO:0032991)	24	RL11; RS11; PICAL; RS20; RS12; RS28; RS16; FA98A; RS27; RS17; RS18; RL36A; RL23A; RL36; RL26; METK2; RS19; PHF5A; RS13; IPP2; RL35A; YKT6; EMC3; GSH0	6	KIF1B; RPN2; TMED2; PSME2; P85A; APOE
membrane (GO:0016020)	4	RAB1A; MAGI3; YKT6; EMC3	8	BST1; PLS3; RPN2; LPP3; RASA1; LPP1; MYO1B; CXA1
extracellular region (GO:0005576)	3	PCOC1; CYR61; PAI1	6	CATL1; COL12; IBP5; TPBG; APOE; WNT5A
extracellular matrix (GO:0031012)	2	PCOC1; CYR61		MMP2; CTHR1; COL12
cell junction (GO:0030054)	1	MAGI3	1	MYO1B
synapse (GO:0045202)	1	PZRN3	0	

Table S6. Protein class ontology analysis of differential proteins performed in PANTHER

protein class		Up-regulation proteins		Down-regulation proteins
nucleic acid binding (PC00171)	29	RL11; RS11; CRIP2; RS20; RS12; PAIRB; RS28; RS16; RL10A; RS27; SCMC2; PURB; RS17; RS18; RL36A; RL23A; ORN; EI2BG; RL36; LRRF1; RL26; RS24; RS19; ARFG1; CHSP1; RS13; RL35A; RS3A; GNL3	9	SMC1A; M2OM; PDCD4; UBF1; H2AY; MCAT; BZW2; H4; MPCP
hydrolase (PC00121)	12	LYOX; PCOC1; VCAM1; PPME1; LYPA2; SERB; ARSB; ORN; 2AAB; THRB; PA24A; GNL3;	9	SMC1A; BST1; CATL1; CN37; LPP3; LPP1; GLO2; CNTN2; NT5D2
enzyme modulator (PC00095)	11	PDCL3; GMFB; PCOC1; ARHG6; EI2BG; RHOA; FSTL1; PAI1; ARFG1; IPP2; GNL3	4	CAV1; RASA1; P85A; MYO1B
signalling molecule (PC00207)	9	GMFB; FGF2; PCOC1; ARHG6; S10AB; CYR61; SDC2; OLR1; GNL3	4	MGP; UBF1; WNT5A; PLXA3
transferase (PC00220)	8	TANC1; FPPS; PDXK; EI2BG; HIBCH; METK2; GFPT2; MAGI3	6	THTM; MRCKA; RPN2; MAGT1; AAK1; HMGCL
oxidoreductase (PC00176)	6	LYOX; PCOC1; ERG; HIBCH; DYR; ADAS	5	AL3A1; CATA; CTHR1; DHI1; COX7C
receptor (PC00197)	5	LYOX; PCOC1; VCAM1; MCTS1; VLDLR	6	NTRI; ANTR1; MEP50; TPBG; CNTN2; PLXA3
cytoskeletal protein (PC00085)	4	CRIP2; TPM2; SDC2; TCTP	9	KIF1B; K2C1; ADDG; MARE2; DTNB; K2C4; SPTN2; ADDA; MYO1B
ligase (PC00142)	4	HIBCH; CYBP; ATIF1; GSH0	0	
transfer/carrier protein (PC00219)	4	PCOC1; SCMC2; HBB1; HBA	8	THTM; M2OM; PLS3; ALBU; SFXN3; TMED2; MCAT; MPCP
transporter (PC00227)	4	CGRE1; PCOC1; SCMC2; AT1B1	7	M2OM; VDAC2; SFXN3; VDAC3; ABCD3; MCAT; MPCP
calcium-binding protein (PC00060)	3	SSRA; S10AB; SCMC2	4	M2OM; MGP; MCAT; MPCP

cell adhesion molecule (PC00069)	3	PCOC1; VCAM1; SDC2	1	CNTN2
defence/immunity protein (PC00090)	3	VCAM1; SFTPA; SDC2	1	CNTN2
extracellular matrix protein (PC00102)	3	PCOC1; SDC2; VLDLR	3	MGP; COL12; TPBG
membrane traffic protein (PC00150)	3	PICAL; SSRA; YKT6	2	CAV1; TMED2
transcription factor (PC00218)	3	CRIP2; PURB; LRRF1	1	UBF1
chaperone (PC00072)	2	PDCL3; TBCA	1	TBCE
lyase (PC00144)	2	CGL; HIBCH	2	BST1; HMGCL
cell junction protein (PC00070)	1	MAGI3	2	MYO1B; CXA1
isomerase (PC00135)	1	HIBCH	0	
surfactant (PC00212)	1	SFTPA	0	
transmembrane receptor regulatory/adaptor protein (PC00226)	1	GRB10	1	CAV1
structural protein (PC00211)	0		4	CAV1; K2C1; MGP; K2C4

Table S7. Pathway analysis of differential proteins performed in PANTHER

Pathway analysis	Up-regulation proteins		Down-regulation proteins	
Integrin signalling pathway (P00034)	8	CO2A1; COBA1; CO3A1; RHOA; CO5A1; ARFG1; CO1A1; CO1A2	2	CAV1; P85A
Angiogenesis (P00005)	4	FGF2; PAR1; RHOA; PA24A	3	RASA1; P85A; WNT5A
Blood coagulation (P00011)	3	PAR1; THRB; PAI1	0	
CCKR signalling map (P06959)	3	RHOA; PAI1; PA24A	1	P85A
Cholesterol biosynthesis (P00014)	3	FPPS; FDFT; ERG1	0	
p53 pathway (P00059)	3	SUMO2; PAI1; SUMO3	1	P85A
FGF signalling pathway (P00021)	2	FGF2; 2AAB	1	RASA1
Gonadotropin-releasing hormone receptor pathway (P06664)	2	GTR1; PA24A	2	CAV1; P85A
Inflammation mediated by chemokine and cytokine signalling pathway (P00031)	2	RHOA; PA24A	0	
Alzheimer disease-presenilin pathway (P00004)	1	FSTL1	2	MMP2; WNT5A
Angiotensin II-stimulated signalling through G proteins and beta-arrestin (P05911)	1	RHOA	0	
Apoptosis signalling pathway (P00006)	1	GRP78	0	
Axon guidance mediated by semaphorins (P00007)	1	RHOA	0	
Cadherin signalling pathway (P00012)	1	FSTL1	2	CSK21; WNT5A
Endothelin signalling pathway (P00019)	1	PA24A	1	P85A
Formyltetrahydroformate biosynthesis (P02743)	1	DYR	0	
Heterotrimeric G-protein signalling pathway-Gq alpha and Go alpha mediated pathway (P00027)	1	RHOA	0	

Methionine biosynthesis (P02753)	1	CGL	0	
N-acetylglucosamine metabolism (P02756)	1	GFPT2	0	
O-antigen biosynthesis (P02757)	1	GFPT2	0	
Oxidative stress response (P00046)	1	PA24A	0	
Parkinson disease (P00049)	1	GRP78	1	CSK21
Plasminogen activating cascade (P00050)	1	PAI1	0	
Pyridoxal phosphate salvage pathway (P02770)	1	PDXK	0	
Ras Pathway (P04393)	1	RHOA	0	
S-adenosylmethionine biosynthesis (P02773)	1	METK2	0	
Serine glycine biosynthesis (P02776)	1	SERB	0	
Tetrahydrofolate biosynthesis (P02742)	1	DYR	0	
VEGF signalling pathway (P00056)	1	PA24A	1	P85A
Vitamin B6 metabolism (P02787)	1	PDXK	0	
Wnt signalling pathway (P00057)	1	FSTL1	0	
5-Hydroxytryptamine degradation (P04372)	0		1	AL3A1
Alzheimer disease-amyloid secretase pathway (P00003)	0		1	ADA10
Axon guidance mediated by Slit/Robo (P00008)	0		2	SLIT3; SLIT2
Axon guidance mediated by netrin (P00009)	0		1	P85A
Cell cycle (P00013)	0		1	PSME2
EGF receptor signalling pathway (P00018)	0		1	RASA1
Fructose galactose metabolism (P02744)	0		1	HXK1
General transcription by RNA polymerase I (P00022)	0		1	UBF1
Glycolysis (P00024)	0		1	HXK1
Hypoxia response via HIF activation (P00030)	0		1	P85A
Insulin/IGF pathway-mitogen activated protein kinase kinase/MAP kinase cascade (P00032)	0		1	RASA1

Insulin/IGF pathway-protein kinase B signalling cascade (P00033)	0	1	P85A
Nicotinic acetylcholine receptor signalling pathway (P00044)	0	1	MYO1B
Notch signalling pathway (P00045)	0	1	ADA10
PDGF signalling pathway (P00047)	0	2	RASA1; P85A
PI3 kinase pathway (P00048)	0	1	P85A
Pentose phosphate pathway (P02762)	0	1	HXK1
T cell activation (P00053)	0	1	P85A
VEGF signalling pathway (P00056)	0	1	P85A
Wnt signalling pathway (P00057)	0	2	CSK21; WNT5A
p53 pathway feedback loops 2 (P04398)	0	1	P85A